

## Synthesis of Functionalized Flexible and Rigid Polyurethane for Oil Spill Treatment

---

Hadi S. Al-Lami<sup>1\*</sup>, Abdullah A. Al-Khalaf<sup>2</sup>, Abbas F. Abbas<sup>1</sup>

<sup>1</sup>Department of Chemistry, College of Science, University of Basrah, Basrah, Iraq.

<sup>2</sup>State Company for Iron and Steel, Ministry of Industry and Modified Minerals, Basrah, Iraq.

\*Corresponding author: Hadi S. Al-Lami, email: [hadi.abbas@uobasrah.edu.iq](mailto:hadi.abbas@uobasrah.edu.iq)

Received April 13<sup>th</sup>, 2023; Accepted June 1<sup>st</sup>, 2023.

DOI: <http://dx.doi.org/10.29356/jmcs.v68i2.2046>

**Abstract.** To improve the oleophilic and hydrophobic properties of two different types of polyurethane sponge (flexible, FPU, and rigid, RPU) for oil spill cleanup, acrylamido phenyl chalcone palamitamid, a recently synthesized monomer with long chains of linear alkyl groups, was *in situ* crosslinked with divinylbenzene. Grafted PU cubes were characterized by Fourier transform infrared spectroscopy (FTIR) and scanning electron microscopy (SEM). The water sorption of ungrafted FPU and RPU decreased from 18.05 and 15.66 to 7.31 and 7.06 for grafted FPU and RPU, respectively. The effect of oil type on the sorption capacity testing was explored and compared using crude oil, diesel fuel, and water-oil systems. It was found that the crude oil and diesel fuel sorption of grafted FPU and RPU cubes was increased compared with ungrafted FPU and RPU cubes, and the maximum values for adsorption were recorded using crude oil. These results can be explained by increasing the adherent forces between the adsorbent and the oil surface with increasing oil viscosity, and consequently, the oil adsorption increases. The high oil absorption capacity is mainly attributed to the high porosity of the sponges. The modified FPU and RPU cubes can be effectively used in oil and water spill cleanup.

**Keywords:** Oil spill; polyurethane; grafting; crude oil; diesel fuel.

**Resumen.** Para mejorar las propiedades oleófila e hidrofóbica de dos tipos diferentes de esponjas de poliuretano (flexible, FPU y rígida, RPU) para la limpieza de derrames de petróleo, se llevó a cabo una reacción de entrecruzamiento *in situ* con divinilbenceno a partir de acrilamido fenil chalcona palamitamida, un monómero recientemente sintetizado y que contiene cadenas largas de grupos alquilo lineales. Los cubos de PU injertados se caracterizaron mediante espectroscopía infrarroja por transformada de Fourier (FTIR) y microscopía electrónica de barrido (SEM). La sorción de agua de FPU y RPU no injertadas disminuyó desde 18,05 y 15,66 hasta 7,31 y 7,06 para FPU y RPU injertados, respectivamente. Se exploró y comparó el efecto del tipo de petróleo en las pruebas de capacidad de sorción, utilizando petróleo crudo, combustible diesel y mezcla agua-petróleo. Se encontró que la sorción de petróleo crudo y combustible diesel de los cubos de FPU y RPU injertados aumentó en comparación con los cubos de FPU y RPU no injertados, obteniéndose los valores máximos de adsorción para el caso de petróleo crudo. Estos resultados pueden explicarse en base al aumento de las fuerzas de adherencia entre el adsorbente y la superficie del aceite al aumentar la viscosidad del aceite, y como consecuencia la adsorción del aceite aumenta. La alta capacidad de absorción de aceite se atribuye principalmente a la alta porosidad de las esponjas. Los cubos FPU y RPU modificados se pueden utilizar eficazmente en la limpieza de derrames de petróleo y agua.

**Palabras clave:** Derrame de petróleo; poliuretano; injerto; petróleo crudo; combustible diesel.

---

## Introduction

Due to the oil industry's rapid expansion, which includes oil extraction and the creation of its derivatives, as well as the industrial sector's rapid growth, there is now a considerable increase in the volume of oily wastewater. Many activities, such as industrial effluent release, offshore and onshore petroleum industries, and accidental spills, cause petroleum hydrocarbon contamination in water [1,2]. Petroleum hydrocarbons (crude oil, diesel oil, engine oil, etc.) cause many toxic compounds that are potent immunotoxicants and carcinogenic to human beings [3]. Many technologies, such as booms, skimmers, dispersants, bioremediation, in situ burning, and sorbents, were utilized to prevent further environmental damage from oil spills [4-7]. Among the methods mentioned above, adsorption has provoked considerable interest because of its facile operation, low cost, and flexible design [8,9].

In recent years, great attention has been given to the fabrication of highly hydrophobic materials to separate oil and water [10]. Polymers with hydrophobic-oleophilic properties could be used as low-surface-energy materials for the surfaces of oil sorbents. Up to now, some of them, such as polypropylene (PP) and polyurethane (PU), have already been commercialized [11]. Among the typical and extensively used polymers, polyurethane (PU) is one of the front runners in synthetic polymer materials with excellent mechanical strength, high abrasion resistance, toughness, low-temperature flexibility, corrosion resistance, processability, etc., and is applied in coatings, adhesives, fibers, synthetic leather, and several other novel fields. In addition, PU contains alternating hard and soft segments, which are easily "tailored-made" to gain desired performance by altering the types and quantities of isocyanate, polyol, surfactants, catalysts, fillers, and matrices during the manufacturing process or via advanced characterization techniques [12-14].

Recently, commercial sponge adsorbents, including polyurethane (PU) sponges, have attracted great attention for oil-water separation due to their low cost, good flexibility, three-dimensional structure, and facile design [15]. Given their outstanding properties, sponge adsorbents have been developed as alternative adsorbing materials. However, both PU sponges are naturally amphipathic, limiting oil removal from oil-water mixtures [16]. As a result, recent research has focused on modifying the surface of PU sponges to convert the hydrophilic surface to a hydrophobic surface. Such a surface would make the sponge have a high oil adsorption capacity and good water repellency in the separation process of oil and water. To this end, various materials have been selected to decorate the commercial sponges, including hydrophobic polymers [9], hydrophobic nanoparticles [17,18], carbon materials [19-21], and so on. These modification materials could successfully switch the hydrophilic sponge surface to hydrophobic, making the sponge materials promising candidates for oil spill cleanup. To address oil spill cleanup in specific situations, sponge adsorbents with additional properties such as magnetic property, stimuli-responsiveness, and excellent durability under harsh conditions have recently been investigated.

It is essential to create a quick and effective approach for changing the hydrophilic sponge surface to a hydrophobic one to satisfy the application requirement in oil spill remediation [22-24]. Herein, we explore the chemical surface modification of two types of polyurethane (PU) surfaces: flexible polyurethane foam (FPU) and rigid polyurethane foam (RPU) to compare their activity in cleaning oil spills. Utilize graft polymerization to modify polyurethane (PU) surfaces with additional long-chain monomer molecules in the presence of cross-linkers to improve the hydrophobic/oleophilic nature of the surfaces and, as a result, the performance of the surfaces as oil-cleaning sorbents. The sorption capacities of both grafted PU foams were evaluated in water, crude oil, and diesel fuel, and the capacities were compared between the two types of grafted polyurethane (PU).

## Experimental

### Materials

All three Sigma-Aldrich, Merck, and Fluka companies supplied all the chemicals and solvents used in this study. Aris S.p.A., an Italian company, provided the flexible polyurethane (FPU) sponge for commercial use, and rigid polyurethane foam (RPU) was created following the published method [25], and rigid

polyurethane foam (RPU) was prepared as reported in the literature [25]. Both foams were cut to 1 cm<sup>3</sup> before being used. The Zubair Field Operation Division Company (ZFOD) supplied the Iraqi crude oil and diesel fuel.

### Hydrophobic/oleophilic compound

The new pre-prepared hydrophobic/oleophilic acrylamide phenyl chalcone palamitamid monomer [26] was used to be crosslinked by divinylbenzene and *in situ* grafting polymerization on the FPU and RPU foam cubes. Its structure is exhibited in Fig. 1.

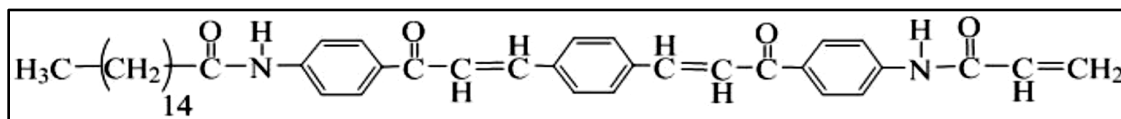
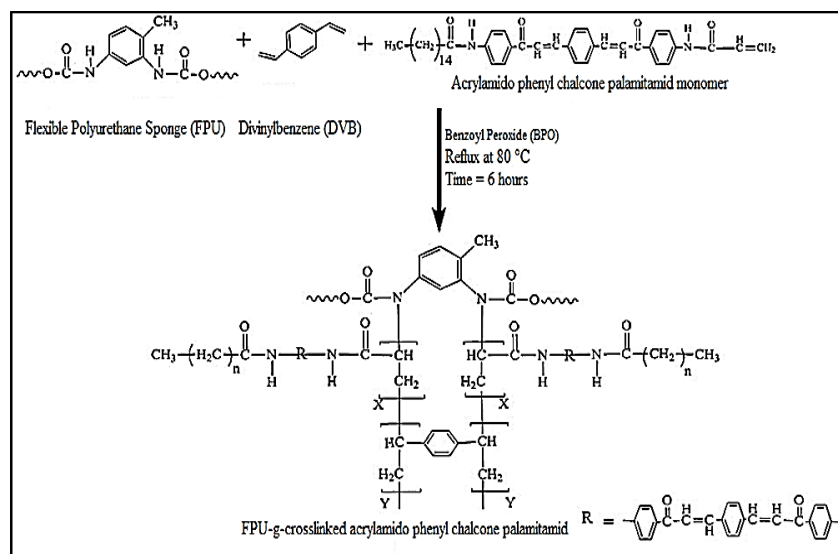


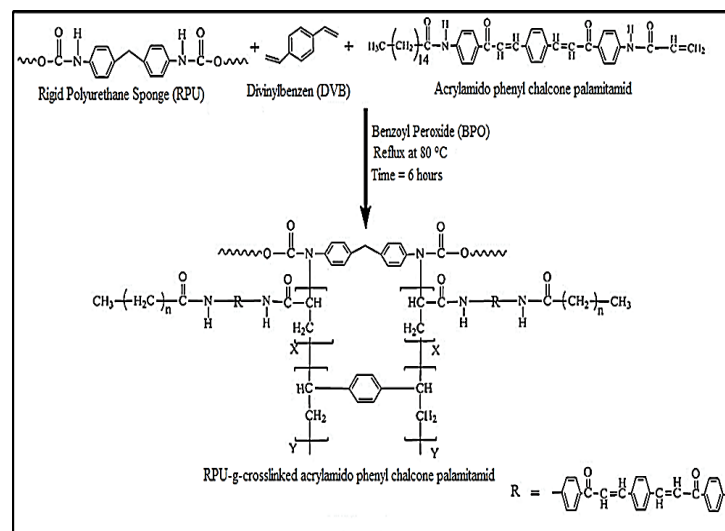
Fig. 1. The chemical structure of the prepared acrylamido phenyl chalcone palamitamid.

### Grafting copolymerization

The *in situ* grafting reaction was performed in a 100-ml three-necked round-bottom flask equipped with a thermometer, nitrogen gas inlet, and reflux condenser. The flask was filled with 0.01 g of the initiator benzoyl peroxide (BPO) dissolved in 50 ml of toluene solvent. 0.2 g of ungrafted flexible polyurethane (FPU) sponge or rigid polyurethane (RPU) foam cubes were immersed in the stirred reactive solution for 20 min at 80 °C. The flask was then filled with a mixture containing 0.3 g of each acrylamide phenyl chalcone palamitamid and 0.003 g of the cross-linker divinylbenzene (DVB). After 6 hours of interaction under stirring (500 rpm) and a nitrogen gas atmosphere at 80 °C, the cubes were washed with ethanol and deionized water several times, then dried at 60 °C under vacuum for 48 hours [25,26]. Schemes 1 and 2 show the grafting reactions of acrylamido phenyl chalcone palamitamid-crosslinked-divinylbenzene onto FPU and RPU, respectively.



Scheme 1. *In situ* grafting polymerization of the prepared crosslinked monomer onto the FPU surface.



**Scheme 2.** *In situ* grafting polymerization of the prepared crosslinked monomer onto the RPU surface.

### Sorption capacity tests

The method improved for the measurement of the oil sorption capacity of the sorbent was based on ASTM F726 2017 Standard Test Method for Sorbent Performance of Adsorbents for use on crude oil and related spills [27,28].

### Water sorption tests

In these tests, the sorbent (FPU or RPU) cubes were initially weighed and then placed into a 100-ml Erlenmeyer flask that contained 50 ml of deionized water. The closed Erlenmeyer flask was then put in a shaker (150 rpm) and shaken for 15 minutes. The contents of the flask were allowed to settle for 2 minutes. The sorbent was removed and allowed to drain for 30 seconds before being immediately transferred to a preweighed Erlenmeyer flask and weighed. The water sorption was calculated using the following equation (1):

$$\text{Water sorption } \left( \frac{g}{g} \right) = \frac{(S_{wt} - S_o)}{S_o} \quad (1)$$

where  $S_o$  is the initial dry weight of the sorbent and  $S_{wt}$  is the wet weight of the sorbent (after water sorption).

### Oil sorption test

For oil sorption tests, crude oil, or diesel fuel (50 ml) was decanted into a 100 ml beaker. The sorbent (FPU or RPU) cubes were weighed, and their value recorded, then they were immersed in crude oil or diesel fuel. In general, after 20 minutes of inundation, the sorbent (FPU or RPU) cubes were removed and allowed to drain for 30 seconds. The saturated sorbent was then immediately transferred to a pre-weighed weighing bottle and weighed. On a weight basis, the oil sorption of sorbent (FPU) cubes was calculated as follows using equation (2):

$$\text{Oil sorption } (g/g) = \frac{(S_t - S_o)}{S_o} \quad (2)$$

where  $S_o$  is the initial dry weight of a sorbent and  $S_t$  is the weight of the sorbent with oil absorbed. Solvent sorption capacity measurements were carried out similarly.

### Oil-water system sorption test

In water–oil system sorption tests, 4.0 g of crude oil or diesel fuel was decanted into a 100 mL Erlenmeyer flask that was filled with 50 mL of deionized water, and the thickness of the oil layer was 2–3 mm.

The sorbent (FPU or RPU) cubes were initially weighed and put into the Erlenmeyer flask. The closed Erlenmeyer flask was then put in a shaker (150 rpm) and shaken for 30 minutes. The contents of the closed Erlenmeyer flask were allowed to settle for 2 minutes. The sorbent (FPU or RPU) cubes were then transferred to an Erlenmeyer flask and extracted several times with petroleum ether (boiling range 30–60 °C); the sorbent was then removed and squeezed to extract the absorbed petroleum ether. Anhydrous sodium sulfate was added to the petroleum ether solution until there was no agglomeration, and then the Erlenmeyer flask was sealed for 30 minutes to dehydrate [27,28]. The oil–water system sorption capacities were obtained using equation (3).

$$\text{Oil – water sorption (g/g)} = \frac{(M_t - M_o)}{S_o} \quad (3)$$

where  $M_o$  is the constant weight beaker,  $M_t$  is the weight of the constant weight beaker with absorbed oil, and  $S_o$  is the initial dry weight of the sorbent.

## Results and discussion

To develop the oleophilic and hydrophobic properties of PU foams, *in situ* grafting polymerization with acrylamido phenyl chalcone palamitamid monomer crosslinked with divinylbenzene was used to modify two types of polyurethane (PU): flexible polyurethane (FPU) and rigid polyurethane (RPU). Fourier transform infrared (Shimadzu FTIR-8400/Japan) and scanning electron microscopy (MIRA3 LMU TESCAN/Czech Republic) were employed to analyze the polyurethane. The testing used crude oil and diesel fuel as oil samples, and the sorption properties of the ungrafted and grafted PU cubes in water, pure oil phase, and water-oil systems were fully investigated and compared. The experiment's data was an average of three experiments.

### FTIR characterization

FTIR analysis confirmed the grafting polymerization of FPU and RPU foams with prepared crosslinked grafted monomers. The reduction in the peak of the isocyanate group of the urethane at  $2368\text{ cm}^{-1}$  in the FTIR spectra implied the correctness of the grafting process. When comparing the infrared spectra of both grafted polyurethane foams (Figures 3 and 5) to the infrared spectra of an ungrafted polyurethane (Figures 2 and 4) we observe a decrease in the strength of the NCO peak that appears at  $2250\text{ cm}^{-1}$ . In addition to an increase in the intensity of each of the  $(\text{CH}_2)$  aliphatic peaks at  $(2866\text{--}2970)\text{ cm}^{-1}$ , the carbonyl group  $(\text{C}=\text{O})$  exhibits a shift from  $1712\text{ cm}^{-1}$  to  $1720\text{ cm}^{-1}$ , as well as an increase in its intensity. These values agreed very well with the results reported in the literature [29,30].

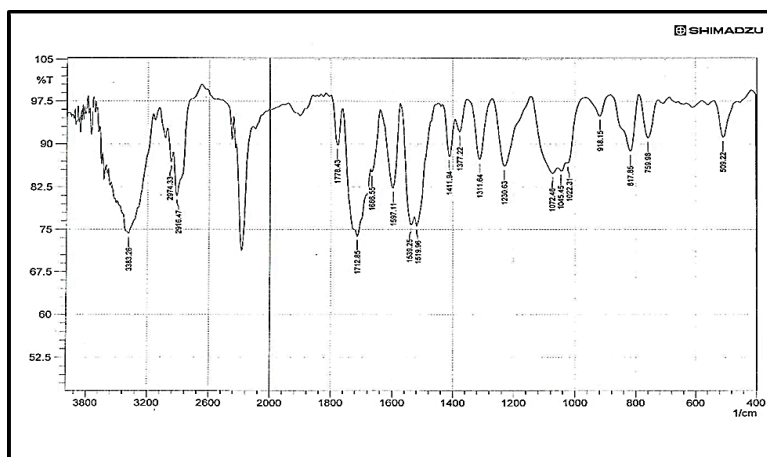
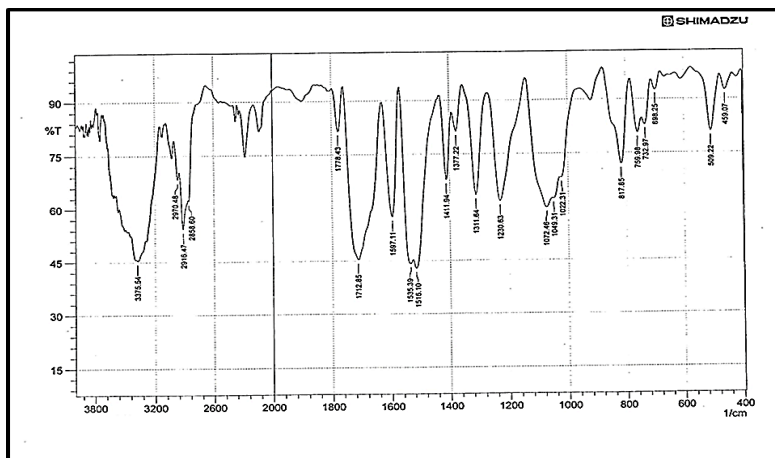
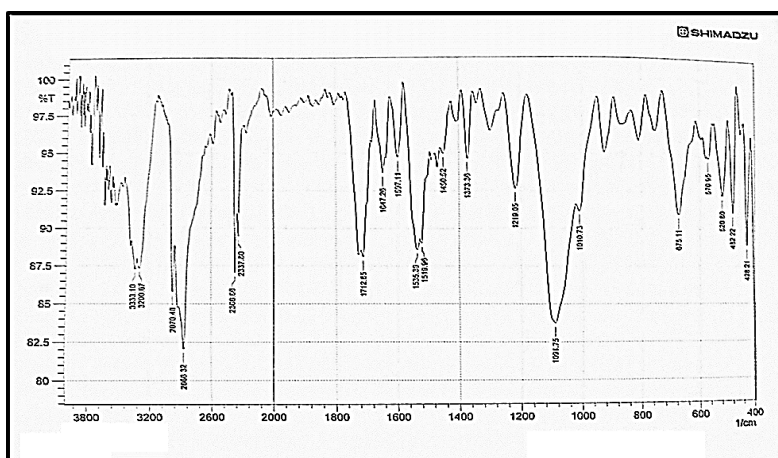


Fig. 2. FTIR spectrum of ungrafted RPU foam.



**Fig. 3.** FTIR spectrum of grafted RPU foam.



**Fig. 4.** FTIR spectrum of ungrafted FPU foam.

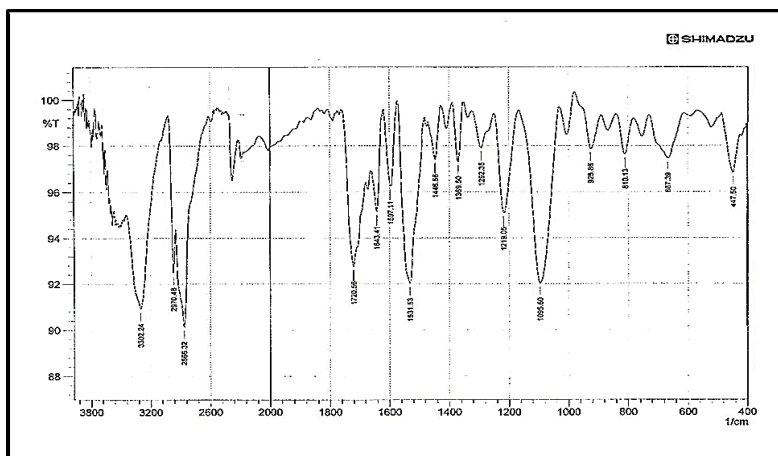


**Fig. 5.** FTIR spectrum of grafted FPU foam.

### SEM characterization

Scanning electron microscopy (SEM) was used to analyze and study the morphological aspects of the ungrafted PU surface and the modified PU surface. From the SEM micrographs of the ungrafted flexible and rigid PU cubes and the grafted flexible and rigid PU cubes shown, the pentagonal cell structure of the ungrafted PU cubes was not ideal.

Fig. 6 shows different magnification ratios of the SEM images of the PU sponges before and after being grafted [31]. The surfaces of the untreated RPU sponges were smooth and flat (Fig. 6(a–c)), and there was no destruction in the RPU cubes. Furthermore, Fig. 7 shows that the *in-situ* crosslinking grafting polymerization destroyed the cell structure and backbone of the PU cubes [28]. The micrographs also show the presence of thin cellular wall films within the foams, which may enhance their surface area, possibly further aiding oil sorption.

There were no obvious micro-scale protrusions or spherical structures distributed on the surfaces at the high magnification shown in Figures 6(a) and 7(a), as well as at low magnification in Figures 6(b), (c) and 7(b), (c). The high-magnification SEM picture also showed that numerous microscopic spherical particles were dispersed on the sponge [32]. The SEM images demonstrated that grafting with the new monomers resulted in the formation of spherical particles on the surface. The spherical particles were very important to the hydrophobicity of the sponges, just like surface protrusions were to the hydrophobicity of lotus leaves [33].

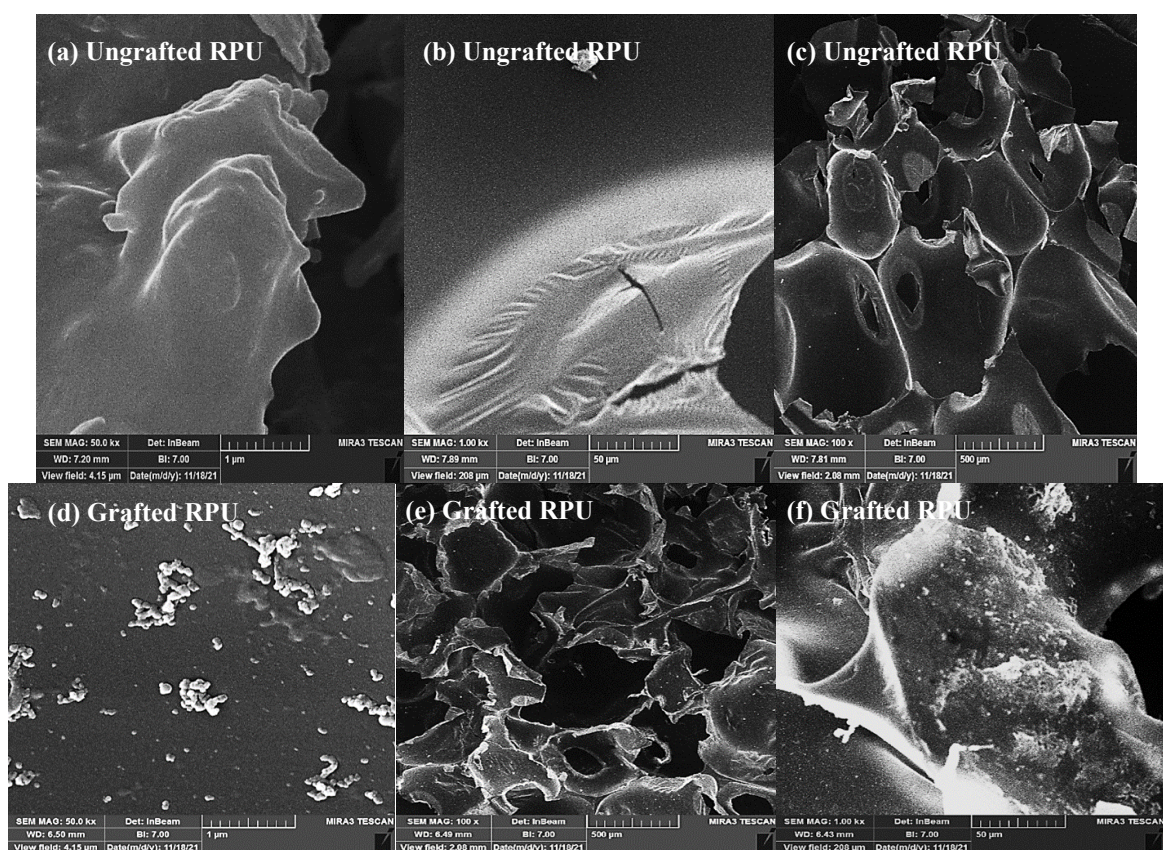
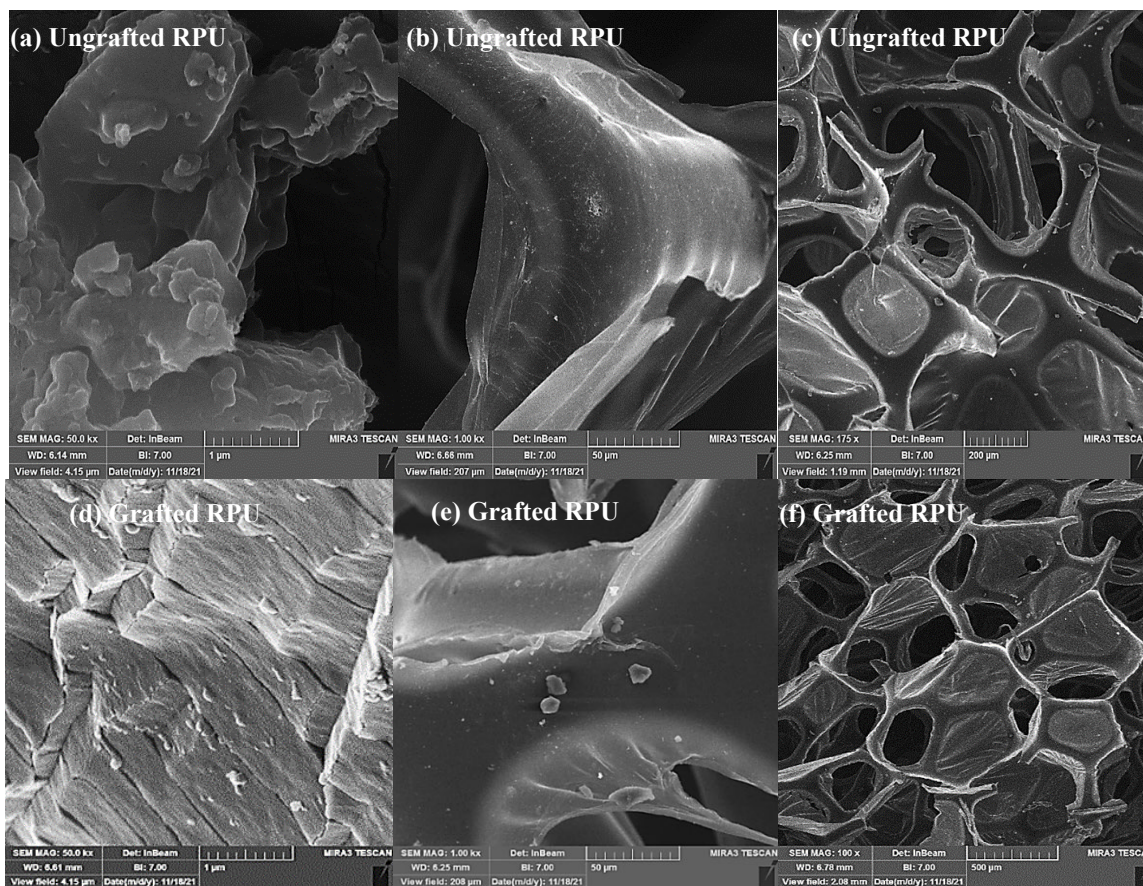


Fig. 6. SEM photographs of the ungrafted RPU cubes (a-c), and grafted RPU (d-f).



**Fig. 7.** SEM photographs of the ungrafted FPU cubes (a-c), and grafted FPU (d-f).

### Water sorption capacity

In water sorption tests, the water sorption was calculated using Equation 1. The results obtained for the water sorption capacity of ungrafted FPU, grafted FPU, ungrafted RPU, and grafted RPU cubes are listed in Table 1 and shown in Fig. 8. The water sorption capacity is found to be higher for ungrafted FPU and RPU cubes compared to the grafted FPU and RPU cubes, where it decreased by about 60 % after the grafting process for the grafted FPU and by about 55 % for the grafted RPU, as shown in Fig. 8. This may be attributed to the long alkyl chains of the crosslinked grafted monomer, which exhibit more oleophilic and less hydrophobic properties simultaneously [34]. This implies that PU cubes grafted with the newly prepared crosslinked monomer were more hydrophobic than ungrafted FPU and RPU cubes. The increase in the hydrophobic properties of the grafted PU cubes may be attributed to the decrease in polarity due to the presence of more non-polar methylene groups in the grafted crosslinked monomer [35].

It was also observed that for both ungrafted and grafted samples, the FPU's absorption capacity is marginally greater than that of the RPU when comparing the two types of polyurethane. This is because flexible polyurethane has heterogeneous pore geometry and pore distribution in contrast to rigid polyurethane, which has rather homogeneous pore geometry and pore distribution [36]. These outcomes match those of the SEM depicted in Figures 6 and 7. When compared to the uneven and poorly dispersed pores of RPU, the pores of FPU are homogeneous and well-distributed. Therefore, samples of FPU grafted and ungrafted will absorb water more than those of RPU grafted and ungrafted.

**Table 1.** The water sorption capacity of the ungrafted and grafted FPU and RPU cubes.

Cube Type	$S_0$ (g)	$S_{wt}$ (g)	Water Sorption Capacity (g/g)	Capacity Ratio (%)
Ungrafted FPU	0.1033	1.9674	18.05	59.50
Grafted FPU	0.1085	0.9012	7.31	
Ungrafted RPU	0.0881	1.4674	15.66	54.92
Grafted RPU	0.0914	0.73592	7.06	

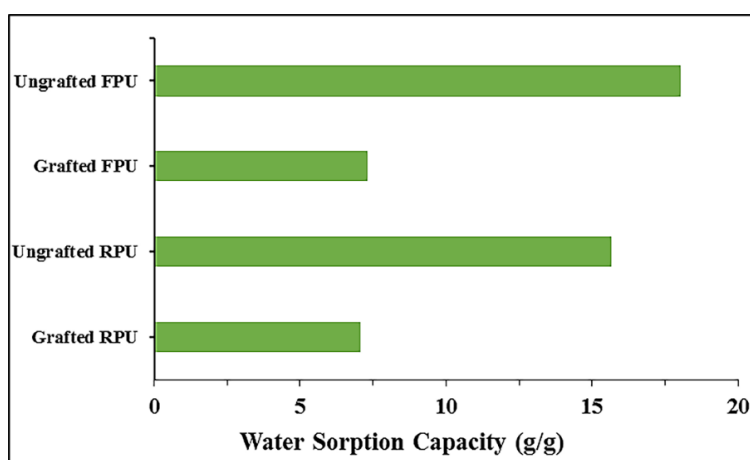


**Fig. 8.** The water sorption capacity of the ungrafted and grafted FPU and RPU cubes.

### Crude oil sorption capacity

The crude oil sorption of both grafted and ungrafted polyurethane foam was calculated using Equation 2. The results of the crude oil absorption capacity of ungrafted FPU and RPU cubes and grafted FPU and RPU cubes obtained are shown in Table 2 and Fig. 9.

The results revealed that *in situ* crosslinking polymerization of the prepared monomer would increase the oleophilicity of both types of tested PU, i.e., RPU and FPU. This effect may be attributed to the effect of the alkyl chain length of the grafted monomer on the porosity of the grafted RPU and FPU, as seen by SEM on the changed PU foam surfaces. The micrographs also show the presence of thin cellular wall films within the foams, which may enhance their surface area, possibly further aiding oil sorption. The particles were generally spherical. However, it can be said that the size distribution for all samples is rather wide. It can be seen that the PU has a porous network structure. This indicates that the crosslinked alkyl chain length of the compounds plays an important role in the capacity of the grafted RPU and FPU foam for crude oil absorbency. Increasing the number of CH<sub>2</sub> groups in the alkyl chain length resulted in better crude oil sorption capacity due to the increasing hydrophobicity properties [37].

**Table 2.** The crude oil sorption capacity of the ungrafted and grafted FPU and RPU cubes.

Cube Type	$S_o$ (g)	$S_{co}$ (g)	Crude Oil Sorption Capacity (g/g)	Capacity Ratio (%)
Ungrafted FPU	0.0916	2.7536	29.06	40.46
Grafted FPU	0.1055	5.255	48.81	
Ungrafted RPU	0.1360	3.1587	22.23	46.10
Grafted RPU	0.1062	4.4861	41.24	

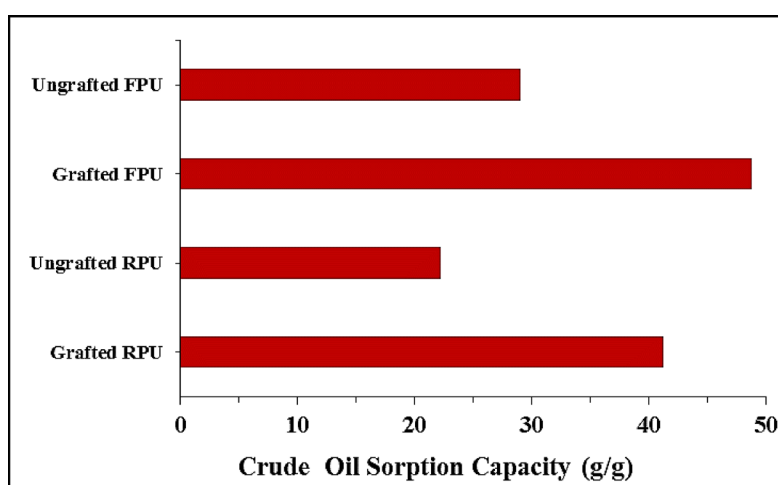


**Fig. 9.** The crude oil sorption capacity of the ungrafted and grafted FPU and RPU cubes.

### Diesel fuel sorption capacity

The diesel fuel sorption capacities of ungrafted FPU and RPU cubes and grafted FPU and RPU cubes are calculated using equation 2 and shown in Table 3 and Fig. 10. As expected, grafted (FPU or RPU) cubes showed enhanced performance in absorbing crude oil and diesel fuel, as shown in Figures 2 and 3, in contrast with ungrafted (FPU or RPU) cubes. Comparing the two Tables (2 and 3), perhaps a difference was observed in the absorption ratio between the grafted FPU and RPU cubes for both crude oil and diesel fuel absorption, but it was much higher than the capacity of water absorption (Table 1).

**Table 3.** The diesel fuel sorption capacity of the ungrafted and grafted FPU and RPU cubes.

Cube Type	$S_o$ (g)	$S_{co}$ (g)	Crude Oil Sorption Capacity (g/g)	Capacity Ratio (%)
Ungrafted FPU	0.1082	3.0587	27.27	35.53
Grafted FPU	0.1055	4.7841	42.30	
Ungrafted RPU	0.1060	2.2587	20.31	45.36
Grafted RPU	0.0906	3.4861	837.4	

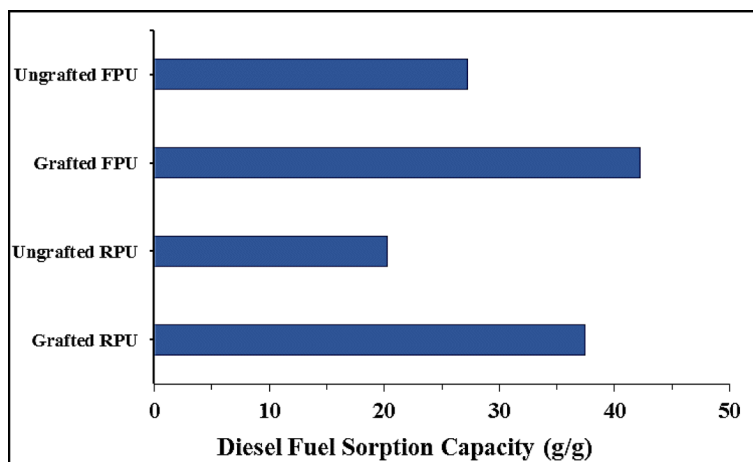


**Fig. 10.** The diesel fuel sorption capacity of the ungrafted and grafted FPU and RPU cubes.

Furthermore, the incorporation of long-chain crosslinked alkyl groups into the PU backbones improves the hydrophobic properties of the FPU or RPU cubes. In contrast, the sorption capacity of the grafted PU cubes for crude oil and diesel fuel increased in a higher manner than that of the ungrafted PU cubes due to the presence of long aliphatic non-polar groups ( $-\text{CH}_3$  and  $-\text{CH}_2$ ). These are hydrophobic groups in nature, and the enhanced oleophilic and hydrophobicity of grafted (FPU or RPU) cubes may be used to explain this [38]. This can be seen clearly in Table 4 and Fig. 12.

**Table 4.** The water, crude oil, and diesel sorption capacities of the ungrafted and grafted FPU and RPU cubes.

Cube Type	Water Sorption (g/g)	Crude Oil Sorption (g/g)	Diesel Fuel Sorption Capacity (g/g)
Ungrafted FPU	18.0454	29.0611	27.27
Grafted FPU	7.3059	48.8104	42.30
Ungrafted RPU	15.6560	22.2257	20.31
Grafted RPU	7.0516	41.2419	37.48

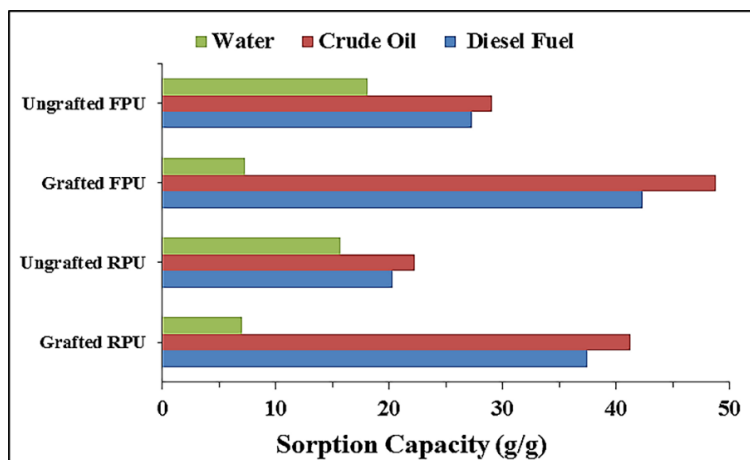


**Fig. 11.** Water, crude oil, and diesel fuel sorption capacities of the ungrafted and grafted FPU and RPU cubes.

### Water-oil system sorption tests

To investigate their sorption capacity in water systems, crude oil, and diesel fuel were accidentally spilled on the water's surface. Grafted and ungrafted FPU and RPU cubes were simply placed on the surface of the oil-water mixture to allow for the collection of oils from the water's surface, which was quickly absorbed, and they were separated from the aqueous phase by removing the cube samples. Their oil sorption capacities in the water–crude oil system and the water–diesel fuel system were calculated using Equation 3.

The results obtained are shown in Table 5 and Fig. 12 and Table 6 and Fig. 13, respectively. The largest crude oil sorption capacity obtained with the grafted FPU was 46.65 g/g, which is greater than the grafted RPU of 38.78 g/g. The same method obtained with a water–diesel fuel system ranged from 36.35 to 34.49 g/g. These results imply that the grafted FPU and RPU were developed to show higher sorption capacities, as shown in the tables and figures above. On the other hand, the results revealed that the hydrophobic surfaces have less interaction with water because of the nonpolar functional groups at the surface. SEM analysis of these outcomes provided support. When crude oil and diesel fuel were cleaned from the water's surface using PU cubes as absorbent materials, they displayed great oil sorption capacity and selectivity by combining special wettability and high porosity.

**Table 5.** The Sorption of water–crude oil system tests the ungrafted and grafted FPU and RPU cubes in the water–crude oil sorption system.

Cube Type	$S_0$	$M_0$	$M_t$	Water-Crude Oil System Sorption Capacity (g/g)	Capacity Ratio (%)
Ungrafted FPU	0.1033	43.2935	46.1122	27.29	41.50
Grafted FPU	0.1096	43.2935	48.4064	46.65	
Ungrafted RPU	0.1051	43.2935	45.6561	22.48	42.03
Grafted RPU	0.136	43.2935	48.5675	38.78	

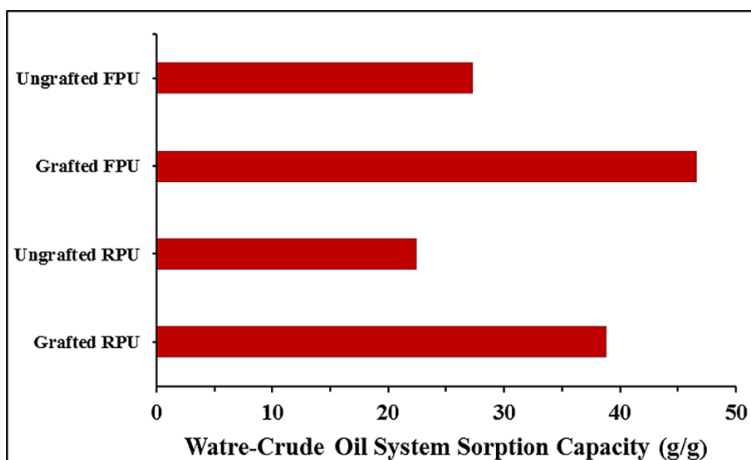


**Fig. 12.** The crude oil sorption capacity in the water–crude oil system of the ungrafted and grafted FPU and RPU cubes.

**Table 6.** The sorption of water–diesel fuel system capacities of the ungrafted and grafted FPU and RPU cubes in a water–diesel fuel sorption system.

Cube Type	$S_o$	$M_o$	$M_t$	Water-Diesel Fuel System Sorption Capacity (g/g)	Capacity Ratio (%)
Ungrafted FPU	0.1033	43.2935	45.5954	22.28	38.71
Grafted FPU	0.1096	43.2935	47.2776	36.35	
Ungrafted RPU	0.1023	43.2935	45.3643	20.24	41.32
Grafted RPU	0.109	43.2935	47.0530	34.49	

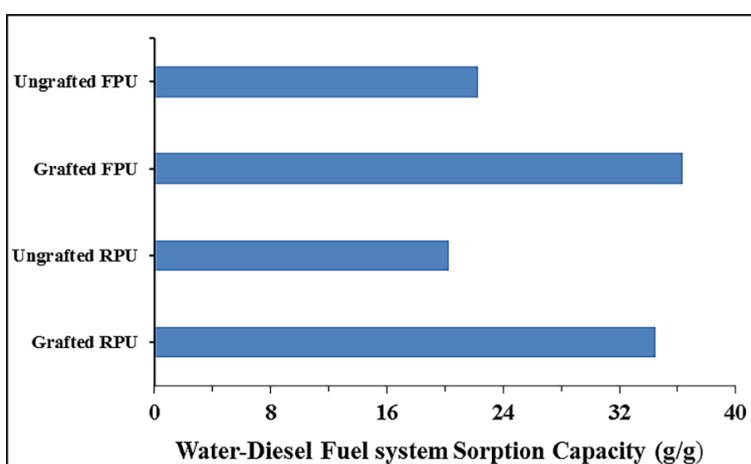


**Fig. 13.** The diesel fuel sorption capacity in water–diesel fuel system of the ungrafted and grafted FPU and RPU cubes.

### Effect of the water-oil type on the sorption capacities

The effect of oil type on oil sorption capacity using water-crude oil and water-diesel fuel systems can be demonstrated in Table 6 and Fig. 14. Both crude oil and diesel fuel have maximum sorption capacities, with crude oil having the best value. Oil adsorption increases as oil viscosity increases because of the adhering forces between the adsorbent and the oil surface. The PU cube's excellent capacity to absorb oil is due to its high porosity. Oil was stored in the pores thanks to the attraction forces between the oil and the grafted FPU and RPU. The sponge was filled with many holes that let water pass through. The exceptional oil absorption capacity of the PU cubes is partly due to their high porosity.

Oil was able to be stored in the pores due to the forces of attraction between it and the grafted cubes. Therefore, oil was able to reach a greater level. The entire structure could be thought of as capillary walls, and these holes are roughly equivalent to capillaries. Because crude oil and diesel fuel have viscosities that are higher than the viscosity of water, there may be a differential in the sorption capacities of the two substances in their respective water systems. The competition between water and both crude oil and diesel fuel at the sponge's surface is heightened, which lowers the amount of each liquid that is absorbed compared to when each liquid is alone.

**Table 6.** The water-crude oil, and water-diesel sorption system capacities of the ungrafted and grafted FPU and RPU cubes.

Cube Type	Water-Crude Oil System Sorption Capacity (g/g)	Water-Diesel Fuel System Sorption Capacity (g/g)
Ungrafted FPU	29.0611	27.27
Grafted FPU	48.8104	42.30
Ungrafted RPU	22.2257	20.31
Grafted RPU	41.2419	37.48

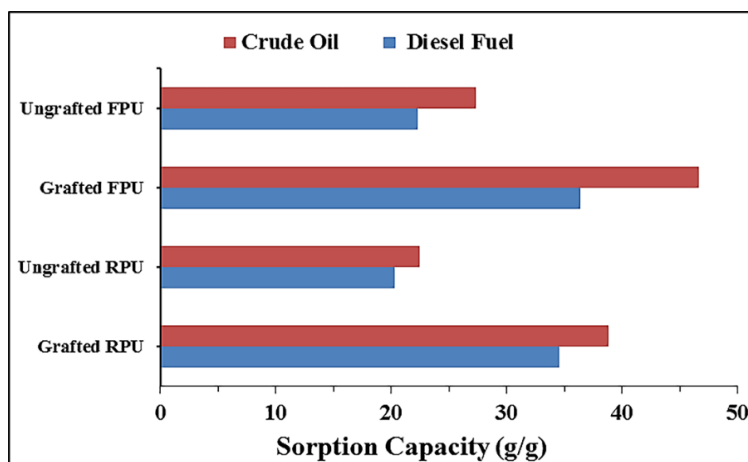


**Fig. 14.** The sorption of water-crude oil and water-diesel fuel systems of the ungrafted and grafted FPU and RPU cubes.

### Conclusions

Commercial FPU and prepared RPU cubes were successfully grafted by in situ polymerization with an oleophilic/hydrophobic crosslinked monomer based on the prepared acrylamido phenyl chalcone

palamitamid. Oils were collected from the surface of the water by simply placing ungrafted and grafted (FPU and RPU) cubes on the surface of the crude oil-water mixture and the diesel fuel-water mixture. The oil sorption of modified FPU and RPU cubes was enhanced, especially in the water-oil system, meeting the challenge for environmental protection of marine systems and aqueous ecosystems. When compared to ungrafted FPU and RPU cubes, the grafting modification reduced the water sorption capacity by 60 % and 55 %, respectively. The crude oil sorption and diesel fuel sorption capacities of grafted FPU were increased from 29.06 to 48.81 g/g and from 27.27 to 42.30 g/g, respectively, compared to ungrafted FPU, while grafted RPU increased from 22.23 to 41.24 g/g and from 20.31 to 37.84 g/g for diesel fuel, respectively. In the water-crude oil system, compared with ungrafted FPU and RPU cubes of 27.29 g/g for FPU and 22.48 g/g. The hydrophobic polyurethane sponges described here might be a potential absorptive material for the cleanup of water-oil spills due to their simplicity of manufacture, good commercial availability of raw materials, and outstanding reusability.

## Acknowledgements

The authors would like to thank the Department of Chemistry, College of Science, at the University of Basrah for their assistance. Without their exceptional assistance, this paper and the research results behind it would not have been possible.

## References

1. Peterson, C. H.; Rice, S. D.; Short, J. W.; Esler, D.; Bodkin, J. L.; Ballachey, B. E.; Irons, D.B. *Science*. **2003**, 302, 2082–2086. DOI: <https://doi.org/10.1126/science.1084282>.
2. Bidgoli, H.; Khodadadi, A.A.; Mortazavi, Y. *J. Environ. Chem. Eng.* **2019**, 7, 103340. DOI: <https://doi.org/10.1016/j.jece.2019.103340>.
3. Liu, Y.; Wang, X.; Feng S. *Adv. Funct. Mater.* **2019**, 29, 1902488. DOI: <https://doi.org/10.1002/adfm.201902488>.
4. Benner, S. W.; John, V. T.; Hall, C. K. *J. Phys. Chem.* **2015**, 119, 6979-6990. DOI: <https://doi.org/10.1021/acs.jpcc.5b01092>.
5. Kim, H.; Zhang, G., Chung, T. M., Nam, C. *Adv. Sustainable Syst.* **2022**, 6, 2100211. DOI: <https://doi.org/10.1002/adsu.202100211>.
6. Muriel, D. F.; Katz, J.; *Langmuir*. 2021, 37, 1725-1742. DOI: <https://doi.org/10.1021/acs.langmuir.0c02986>.
7. Baharuddin, S. H.; Mustahil, N. A.; Reddy, A. V. B.; Abdullah, A.A.; Mutalib, M. I. A.; Moniruzzaman, M. *Chemosphere*. **2020**, 249, 126125. DOI: <https://doi.org/10.1016/j.chemosphere.2020.126125>.
8. Lü, X.; Cui, Z.; Wei, W.; Xie, J.; Liang, J.; Huang, J.; Liu, J. *Chem. Eng. J.* **2016**, 284, 478–486. DOI: <https://doi.org/10.1016/j.cej.2015.09.002>.
9. Peng, M.; Zhu, Y.; Li, H.; He, K.; Zeng, G.; Chen, A.; Chen, G. *Chem. Eng. J.* **2019**, 373, 213-226. DOI: <https://doi.org/10.1016/j.cej.2019.05.013>.
10. Mao, M.; Xu, H.; Guo, K. -Y.; Zhang, J. -W.; Xia, Q. -Q.; Zhang, G. -D.; Zhao, L.; Gao, J. -F.; Tang, L. -C. *Appl. Sci. Manuf.* **2021**, 140, 106191. DOI: <https://doi.org/10.1016/j.compositesa.2020.106191>.
11. Ge, J.; Zhao, H. Y.; Zhu, H.W.; Huang, J.; Shi, L. A.; Yu, S. H. *Adv. Mater.* **2016**, 28, 10459-10490. DOI: <https://doi.org/10.1002/adma.201601812>.
12. Peponi, L.; Puglia, D.; Torre, L.; Valentini, L.; Kenny, J. M. *Mater. Sci. Eng. Reports*. **2014**, 85, 1–46. DOI: <https://dx.doi.org/10.1016/j.msere.2014.08.002>.
13. Tian, S. *Polymers*. **2020**, 12, 1996-2011. DOI: <https://doi.org/10.3390/polym12091996>.
14. Zhu, X.; Li, Q.; Wang, L.; Wang, W.; Liu, S.; Wang, C.; Qian, X. *Eur. Polym. J.* **2021**, 161, 110837. DOI: <https://doi.org/10.1016/j.eurpolymj.2021.110837>.

15. Pham, V. H.; Dickerson, J. H. *ACS Appl. Mater. Interf.* **2014**, *6*, 14181–14188. DOI: <https://doi.org/10.1021/am503503m>.
16. Zhang, W.; Zhai, X.; Xiang, T.; Zhou, M.; Zang, D.; Gao, Z.; Wang, C. *J. Mater. Sci.* **2017**, *52*, 73–85. DOI: <https://doi.org/10.1007/s10853-016-0235-7>.
17. Lei, Z.; Zhang, G.; Ouyang, Y.; Liang, Y.; Deng, Y.; Wang, C. *Mater. Lett.* **2017**, *190*, 119–122. DOI: <https://doi.org/10.1016/J.MATLET.2016.12.082>.
18. Cho, E. C.; Chang-Jian, C. W.; Hsiao, Y.S.; Lee, K. C.; Huang, J. H. *J. Taiwan Inst. Chem. Eng.* **2016**, *67*, 476–483. DOI: <https://doi.org/10.1016/j.jtice.2016.08.002>.
19. He, K.; Chen, G.; Zeng, G.; Chen, A.; Huang, Z.; Shi, J.; Huang, T.; Peng, M.; Hu, L. *Appl. Catal.* **2018**, *228*, 19–28. DOI: <https://doi.org/10.1016/j.apcatb.2018.01.061>.
20. Shiu, R. F.; Lee, C. L.; Hsieh, P. Y.; Chen, C. S.; Kang, Y. Y.; Chin, W. C.; Tai, N. H. *Chemosphere.* **2018**, *207*, 110–117. DOI: <https://doi.org/10.1016/j.chemosphere.2018.05.071>
21. Bagoole, O.; Rahman, M. M.; Shah, S.; Hong, H.; Chen, H.; Ghaferi, A. A.; Younes, H. *Environ. Sci. Pollut. Res. Int.* **2018**, *25*, 23091–23105. DOI: <https://doi.org/10.1007/s11356-018-2248-z>.
22. Wang, H.; Zhang, C.; Zhou, B.; Zhang, Z.; Shen, J.; Du, A. *ACS Appl. Nano Mater.* **2020**, *3*, 1479–1488. DOI: <https://doi.org/10.1021/acsnm.9b02303>.
23. Khosravi, M.; Azizian, S. *ACS Appl. Mater. Interf.* **2015**, *7*, 25326. DOI: <https://doi.org/10.1021/acsnm.5b07504>.
24. Oribayo, O.; Pan, Q.; Feng, X.; Rempel, G. L. *AIChE J.* **2017**, *63*, 4090–4102. DOI: <https://doi.org/10.1002/aic.15767>.
25. Borreguero, A. M.; Valverde, J. L.; Peijs, T.; Rodríguez, J. F.; Carmona, M. *J. Mater. Sci.* **2010**, *45*, 4462–4469. DOI: <https://doi.org/10.1007/s10853-010-4529-x>.
26. Al-Khalaf, A. A.; Abbas, A. F.; Al-Lami, H. S. *Basrah J. Sci.* **2022**, *40*, 437–464. DOI: <https://doi.org/10.29072/basjs.20220214>.
27. Bazargan, A.; Tan, J.; McKay, G. *J. Test. Evalu.* **2015**, *43*, 1271–1278. DOI: <https://doi.org/10.1520/JTE20140227>.
28. Li, H.; Liu, L.; Yang, F. *Mar. Pollut. Bull.* **2012**, *64*, 1648–1653. DOI: <https://doi.org/10.1016/j.marpolbul.2012.05.039>.
29. Wong, C. S.; Badri, K. H. *Mat. Sci. Appl.* **2012**, *3*, 78–86. DOI: <https://doi.org/10.4236/msa.2012.32012>.
30. Selvam, R.; Subramanian, K. *Adv. Polym. Technol.* **2018**, *37*, 724–731. DOI: <https://doi.org/10.1002/adv.21714>.
31. Peng, L.; Yuan, S.; Yan, G.; Yu, P.; Luo, Y. *J. Appl. Polym. Sci.* **2014**, *131*, 40886. DOI: <https://doi.org/10.1002/app.40886>.
32. Keshawy, M.; Farag, R. K.; Gaffer, A. *Egypt. J. Pet.* **2020**, *29*, 67–73. DOI: <https://doi.org/10.1016/j.ejpe.2019.11.001>.
33. Zhang, Y. L.; Xia, H.; Kim, E.; Sun, H. B. *Soft Matter.* **2012**, *8*, 11217–11231. DOI: <https://doi.org/10.1039/c2sm26517f>.
34. Zhu, J.; Wang, Z.; Ni, H.; Liu, X.; Ma, J.; Du, J. *J. Chem.* **2016**, *2016*, 1–7. DOI: <https://doi.org/10.1155/2016/6095023>.
35. Reichardt, C.; Welton, T. in: *Solvents and Solvent Effects in Organic Chemistry*, 4th ed. Wiley-Vch Verlag GmbH & Co. KgaA, Weinheim, **2010**. DOI: <https://doi.org/10.1002/9783527632220>.
36. Blazejczyk, A.; Wierzbicka, P. *Polimery-Warsaw.* **2018**, *63*, 685–693. DOI: <https://doi.org/10.14314/polimery.2018.10.4>.
37. Al-Khalaf, A. A.; Al-Lami, H. S.; Abbas, A. F. *Pet. Sci. Technol.* **2022**, 1–16. DOI: <https://doi.org/10.1080/10916466.2022.2118774>.
38. Visco, A.; Quattrocchi, A.; Nocita, D.; Montanini, R.; Pistone, A. *Nanomaterials.* **2021**, *11*, 735–749. DOI: <https://doi.org/10.3390/nano11030735>.